SIMULATING INTERFERENCE EFFECT BETWEEN REINJECTION WELLS

Marastio, F. E. [1], Hastriansyah, G.[1], Saputra, M. B.[1], Arifin, M. T. [1], Pasaribu, F. [1], and Silaban, M. S. P. [1]

[1]PT. Pertamina Geothermal Energy, Skyline Building 19th Floor, Jakarta, Indonesia

fadiel.marastio@pertamina.com

Keywords: *Interference, Transient, Injection Well, Injection Capacity.*

ABSTRACT

Ensuring the performance of reinjection wells is important for the sustainability of geothermal field management. One of the problems that is rarely noticed in the reinjection performance is the interference-effect. The interference-effect could cause a significant drop in injection well capacity.

Two reinjection wells were suspected of having interconnected fracture permeability and bounded reservoir. Although the distance between the feed zone is more than 300 meters, Well D-2 experienced a temperature drop and pressure increase during the Injectivity Test of Well D-3. A method to estimate optimum total reinjection capacity is delivered.

The approach is using the nodal analysis to obtain each wells' reinjection capacity. Then, analytical and semi-numerical transient models are used to obtain reservoir properties also to simulate the optimum reinjection capacity due to the interference-effect.

1. INTRODUCTION

1.1 Backgrounds

Hululais Geothermal Field is one of the project developments of PT. Pertamina Geothermal Energy which is located at Rejang Lebong Region, Bengkulu Province, Indonesia. It is situated at the Western to Southern side of Sumatran Fault System (SFS), trending relatively NW-SE and composed of some fault segment system (Koestono, 2015). The reservoir type is Liquid Dominated with temperature ranging from 240ºC – 300ºC and the permeability spreading from low to high. The field will be expected to generate electricity for 2 x 55 MW_e.

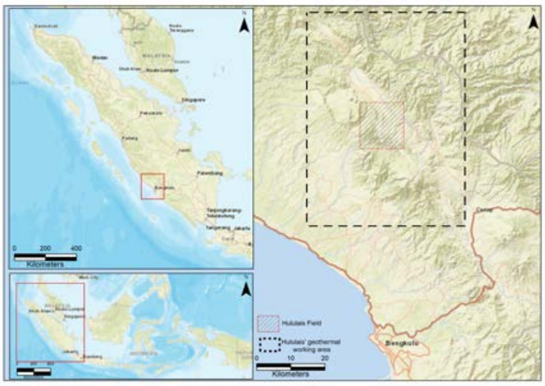

Figure 1: Location of Hululais Field (Topographic was taken from ESRI Database Online, 2020)

Currently, Hululais Field has nine production wells and nine reinjection wells with the total requirement of brine and condensate injection is approximately 3500 ton/hr. In the geothermal field development, the reinjection wells are just as important as the production wells for the sustaining electricity generation. The objectives of reinjection wells in a geothermal reservoir include: disposal of waste-water from power plants and return-water from direct applications; additional recharge to supplement the natural recharge to geothermal systems; pressure support due to reservoir decline because of mass extraction; enhance thermal extraction from reservoir rocks along flow-paths; offset surface subsidence caused by production induced pressure decline; and to enhance or revitalize surface thermal features (Axelsson, 2012; Bromley et, al., 2006).

One of the issues met in the Hululais Field is the interference between reinjection wells. Interference phenomenon is commonly encountered in the highly permeable fractured well. This interference means that there is pressure communication between adjacent wells. High interference in the production wells may cause higher depletion at a point of the reservoir, which is drained from the several wells. Moreover, it might occur in reinjection wells where the injection capacity decreases due to the increase in reservoir pressure at a radius of the well as a result of the simultaneous injecting well.

2. WELL & RESERVOIR CHARACTERISTICS

2.1. Well D-2

Well D-2 is a big hole well with a total depth of 2961 mMD. The well is directed to N 247 E to hit the NW-SE Cemeh Fault. The first loss circulation within the reservoir zone was encountered at 2060 mMD with around 0.6 to 2 bpm and then increased up to 12.8 bpm at the bottom of the well. The total loss circulation only found at 2663 - 2674 mMD. Predominantly altered andesite breccia was observed within the reservoir zone with propylitic alteration type. It was characterized by the occurrence of chlorite, epidote, secondary quartz, pyrite, calcite and low smectite value reflected from low Methylene Blue Test; a test to determine the amount of smectitic swelling clay. The first epidote was encountered at 1053 mMD and then appeared with a trace – slight amount discontinuously to the bottom of the well. The well was stopped at 2961 mMD as the well encountered metasediment.

Well Completion Test, such as PTS Injection, Injectivity Test, Fall-Off Test, PT Heating, was carried out to characterize the well. PTS Injection under 600 gpm injection rates indicated the main feed zone from -750 to -1000 mASL (Fig. 3). An Injectivity Test was conducted to obtain the Injectivity Index. The injection rate started from 4542 lpm (272 t/hr), 3785 lpm (227 t/hr), 3028 lpm (181 t/hr), and 2271 lpm (136 t/hr) with each injection rate held constant for 2 hours. The Injectivity Index of this well is 18.5 t/hr.bar (Fig. 4). Next, the injection rate was increased to 4542 lpm (272 t/hr) for 2 hours and followed by stop pumping for 12 hours to obtain the fall-off transient profile.

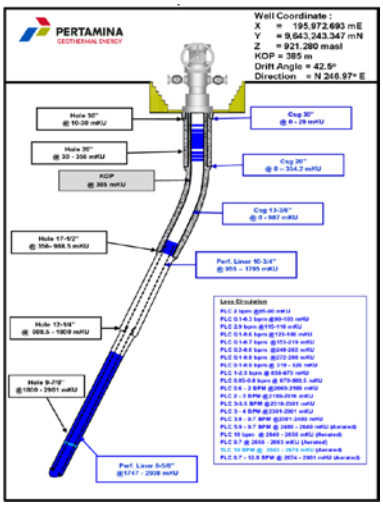

Figure 2: Well Schematic of Well D-2

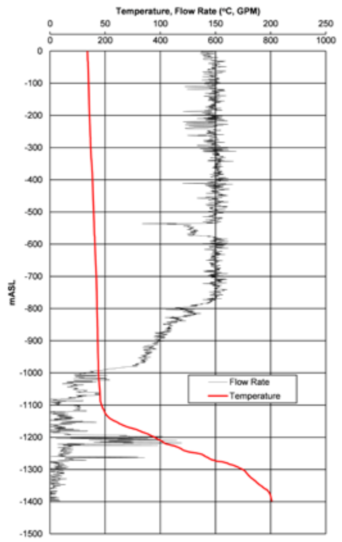

Figure 3: Temperature & Spinner Profile Well D-2 under 600 GPM injection.

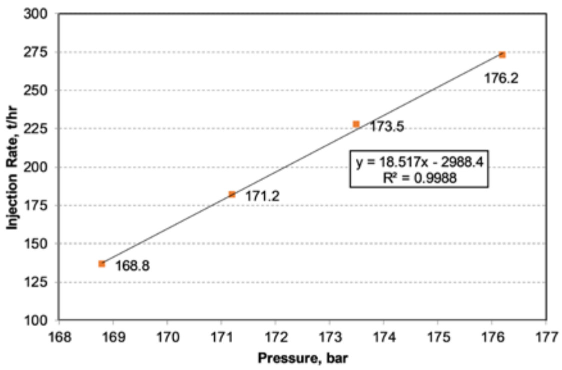

Figure 4: Injectivity Test Well D-2. The Injectivity Index is 18.5 t/h.bar

The transient profile was analyzed using Kappa Workstation v5.2 - Saphir NL. Reservoir and fluid properties for input in the software are seen in Table 1. Reservoir thickness referred to the feed zone thickness from the PTS Injection survey. Total compressibility was a function of rock and liquid compressibility. The analysis used the Saphir default value since it was in order to the water compressibility at the reservoir condition (Meehan, 1980).

Parameter	D-2	D-3
Reservoir thickness, m	250	150
Total compressibility, Pa^{-1}	4.35E-10	
Water viscosity, Pa.s	3.3E-4	
Rock Porosity, fraction	0.1	

Table 1: Reservoir and fluid properties for transient analysis input

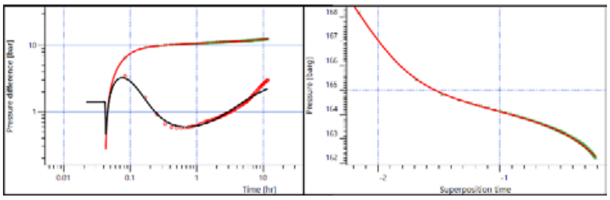

Figure 5: Type Curve Matching Well D-2

Figure 5 shows the transient profile of Well D-2. The apparent profile is at the late time where the pressure derivative is inclining. Its slope tends to change over time, which indicates the flow regime change. The reservoir boundary profile matches with the intersecting fault 54° angle profile.

2.2. Well D-3

Well D-3 was drilled after Well D-2 and targeted to hit the same NW-SE Cemeh Fault. It has a total depth of 2690 mMD. The drilling string got stuck at 2690 mMD due to the hole cleaning problems. Multiple efforts had been made to free the string and the drilling string was cut at 2403 mMD, which left behind 286 m of fish. The lithology in reservoir zone is predominantly altered andesite breccia with secondary quartz, chlorite, pyrite and epidote, lower smectite content reflected from low MBT test. The loss circulation within the reservoir zone was first observed at 2232 mMD (-895 mASL) with 0.3 to 1.7 bpm. The observed loss circulation was increased down to the bottom of the well up to 2.5 to 3.4 bpm.

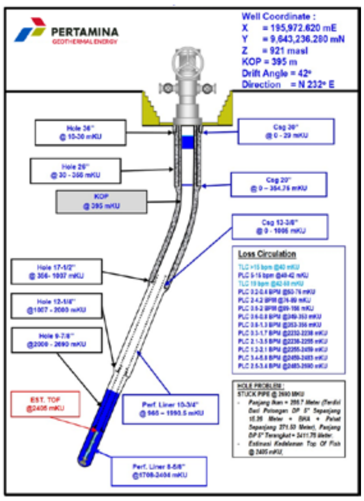

Figure 6: Well Schematic of Well D-3

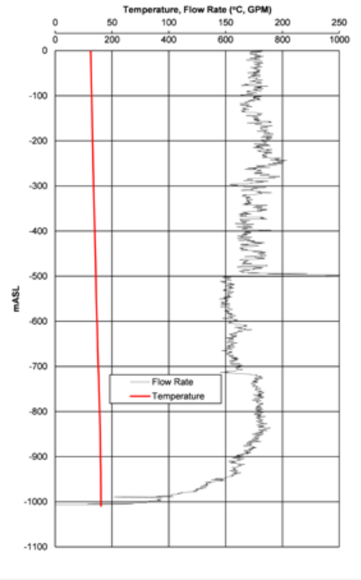

Figure 7: Temperature & Spinner Profile Well D-3 under 700 GPM injection.

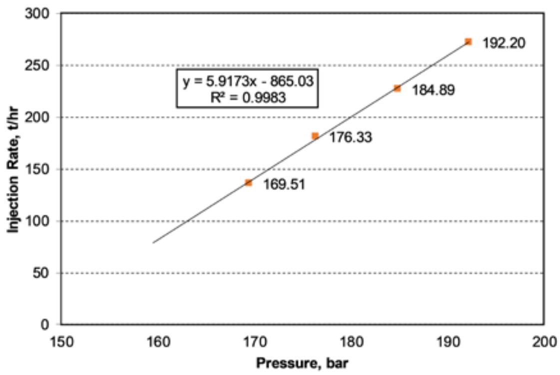

Figure 8: Injectivity Test Well D-3. The Injectivity Index is 5.9 t/hr.bar

Similar to the previous step of Well Completion Test, the Injectivity Index of Well D-3 is 5.9 t/hr.bar. This value much smaller compares to the Well D-2. However, from the PTS Well D-3 profile, the permeable zone is similar to Well D-2 ranging from -860 – -1000 mASL (Fig. 7).

Figure 9 shows the transient profile of Well D-3. In the beginning, the derivative pressure delivers a large hump, which might indicate a higher degree of skin damage. Radial flow also does not appear after 1-½ log cycle. At the late time period, the derivative profile starts to rise, but the short fall-off time might conceal the boundary response. The profile matches with the single fault model. The transient analysis result of Well D-2 and D-3 can be seen in Table 2.

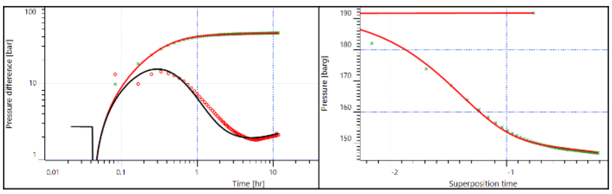

Figure 9: Type Curve Matching Well D-3

Parameter	D-2	D-3
Reservoir Model	Homogeneous	
Reservoir Boundary	Intersecting Fault 54°	Single Fault
Permeability-Thickness, Darcy-m	34.8	10.9
Skin, dimensionless	2.55	4.97
Distance to Fault, meters	207 290	443

Table 2: Pressure transient analysis result

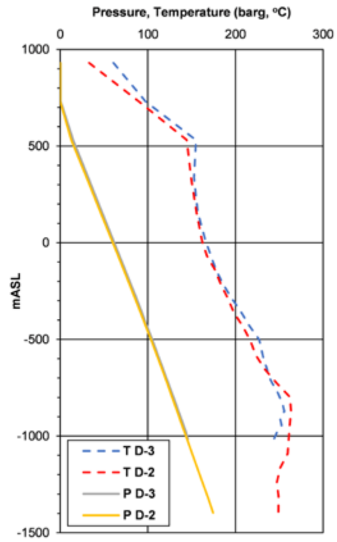

Figure 10: PT Profile Well D-2 and D-3

Figure 10 shows the stabilized pressure and temperature for both wells. The water level, temperature profile, and pressure gradient are similar. The maximum temperature is 263.2°C and 255.7°C for Well D-2 and Well D-3, respectively.

3. INJECTION WELL CAPACITY

Injection well capacity was calculated using an in-house spreadsheet program, Incapa (Hastriansyah, 2015). It performed a nodal analysis, which is an estimation of the optimum flow rate at a given node by combining the Inflow Pressure and the Outflow Pressure. In the producing or injecting well, the node located at the bottom of the well. The Inflow Pressure was the summation of the wellhead pressure, hydrostatic pressure, and the pressure drop along the wellbore. Meanwhile, the Outflow Pressure depends on the reservoir pressure and the reservoir properties which is associated with the Injectivity Index.

Inflow Pressure Equation

$$P_{inj} = P_{wh} + dP_z - dP_f$$

Outflow Pressure Equation

$$P_{inj} = P_{res} + \left(\frac{Q}{II}\right)$$

Where P_{inj} is bottom hole injection pressure, P_{wh} is wellhead pressure, dP_z is hydrostatic pressure, dP_f is frictional pressure drop, P_{res} is reservoir pressure, Q is injection flow rate, and II is injectivity index.

In the calculation, the temperature of the injectate was 40 °C with the wellhead pressure of 0 barg. Stabilized pressure at the main feed zone depth for well D-2 and well D-3 is 162 barg and 147 barg. Figure 11 and 12 shows the optimum injection rate of well D-2 and D-3, which is the intersection of the inflow curve and outflow curve. Well D-2 has 189.14 kg/s or 680.9 ton/hr and D-3 has 80.32 kg/s or 289.16 ton/hr. These results correspond with the Injectivity Index value for each well.

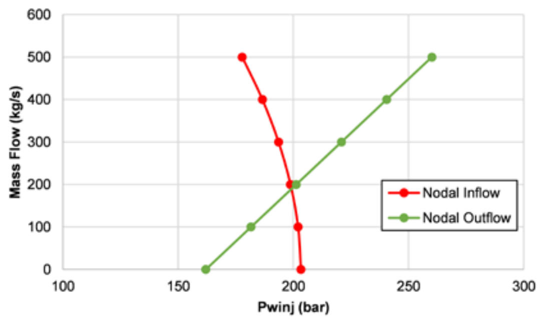

Figure 11: Injection Capacity D-2 with Nodal Analysis. The optimum injection rate under Temp 40°C and WHP 0 barg is 189.1 kg/s or 680.9 ton/hr

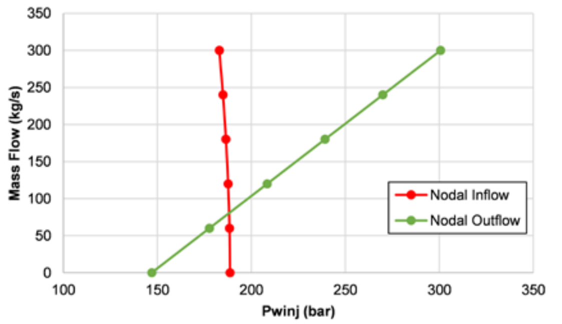

Figure 12: Injection Capacity D-3 with Nodal Analysis. The optimum injection rate under Temp 40°C and WHP 0 barg is 80.3 kg/s or 289.1 ton/hr

4. INTERFERENCE PHENOMENON

During Injection Test in Well D-3, bottom hole pressure and temperature were observed in Well D-2. The earlier assumption was that the 300m distance between the feed zones might not exhibit interference-effect (Fig. 13). Unfortunately, the interference-effect was seen as the pressure rose 3.25 barg and temperature dropped 10 °C to 29°C (Fig. 14). Multiple-well test, such as the interference test or pulse test, was not conducted in this period.

In August 2020, Well D-3 was used for brine disposal from a production well testing. Figure 15 shows a glimpse of recorded data of wellhead pressure Well D-2 and D-3 during three days of injection. During the period, we observed that both wells were in a vacuumed condition. Along the way, the Well D-2 wellhead pressure increased slightly from -0.4 barg to -0.1 barg.

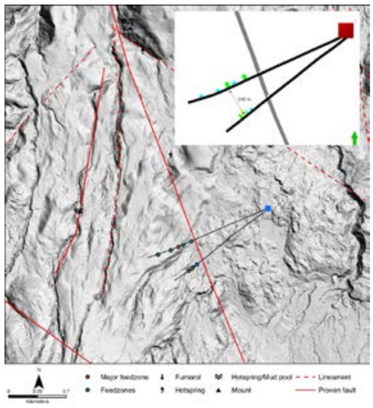

Figure 13: Structure Map of Hululais Field with the location of Well D-2 and Well D-3. The 3D distance between the feed zone is approximately 310 m.

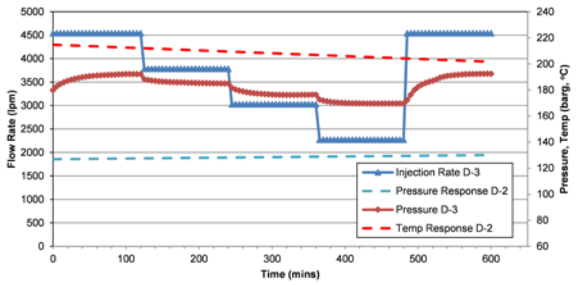

Figure 14: Pressure response of Well D-2 during the Injectivity Test of Well D-3. Pressure increases for 3.25 barg and temperature drops for 10°C

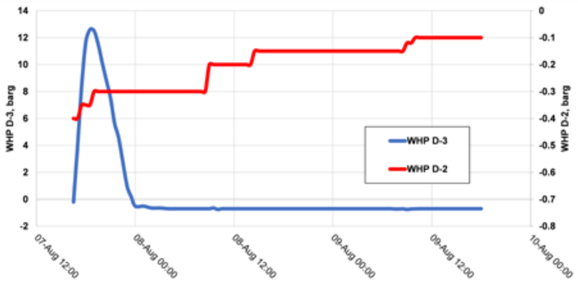

Figure 15: Wellhead Pressure Well D-2 and D-3 during brine injection at Well D-3.

5. INTERFERENCE SIMULATION

5.1. Model Building

A simple reservoir model was developed using Saphir Numerical Analysis. This method neglects the non-isothermal approach that generally applies to a geothermal reservoir. A simplified discrete reservoir model based on the geological map was built using a rectangular Voronoi grid (Fig. 16). There are two impermeable faults seen in the geological model, namely Fault#1 and Fault#2. As the boundary, constant pressure support boundary confines the model. The constant pressure support represents the vast geothermal reservoir, which is supplying fluid encroachment to the wells. Two adjacent impermeable faults were added as the geological feature of the model. For the well placement, it was associated with the major feed zone of those wells. Hence, the simulation occurred at a single point. The near-region and reservoir properties, such as permeability, thickness, and skin, were used as in Table 2. Permeability and thickness distribution are automatically generated from the simulator using the linear regression method. In this case, the Well D-2 was placed as the monitoring and active well. Meanwhile, the Well D-3 became the active well only.

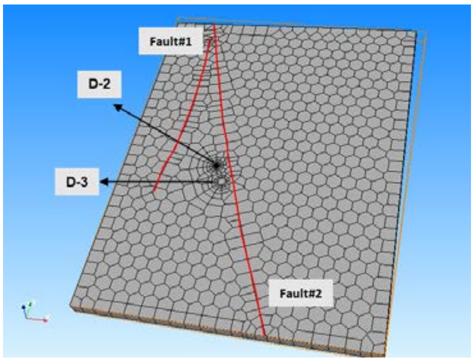

Figure 16: The simulation model.

5.2. Two Wells Injection

After the model was built, two calibration set was conducted to inspect the accuracy of the model. First, the simulation was run to match the Incapa Well D-2 result. Using the same input of Incapa Well D-2, the permeability multiplier had to set to 1.68 to obtain injection pressure at 199.13 barg (Fig. 18).

Second, the completion test scenario was run in the simulator. The initial pressure before the Injectivity Test was 126.7 barg. The simulation result is shown in Figure 17. The simulation data matches the pressure response.

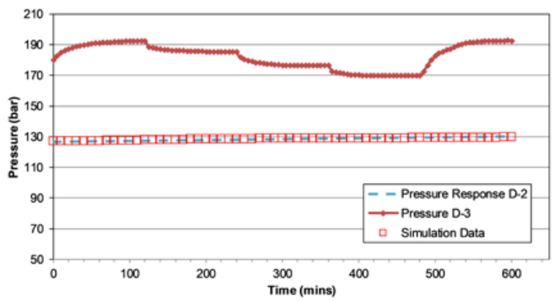

Figure 17: Well D-2 simulation result from the Injectivity Test Well D-3

The calibrated model was used to simulate the optimum injection capacity from two wells. The constraint of the simulation was the injection pressure in the observation well (Well D-2), which set to 199.13 barg. Initial pressure was 162 barg and the injection schedule lasted for 30 days. This method needs manual-user iteration to determine the optimum injection rate.

The first step was to inject both wells with individual injection capacity. The total rate injected into the reservoir was 969 ton/hr (Temp. 40°C). After 30 days of injection, the observed pressure in Well D-2 was 206 barg (Fig. 18). The rate for each well then was optimized individually.

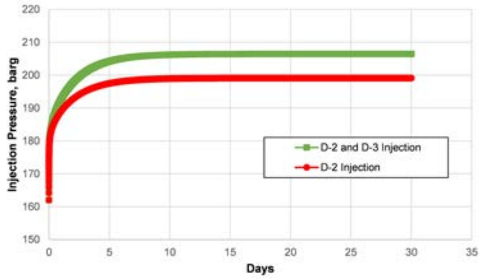

Figure 18: Injection pressure observed in Well D-2. The red line shows the Well D-2 injection to the reservoir with bottom hole pressure 199.1 barg. The green line shows the Well D-2 pressure stabilizes at 206 barg while both Well D-2 and D-3 are injecting simultaneously.

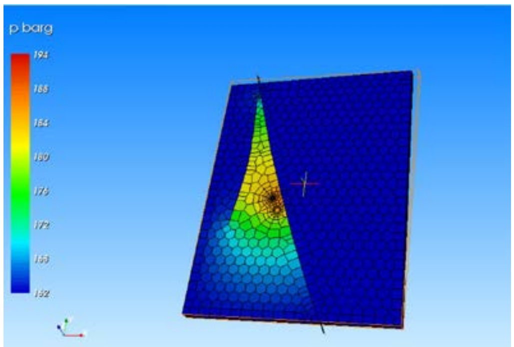

Figure 19: Model pressure distribution where D-2 injects 568 ton/hr and D-3 injects 241 ton/hr

After running several scenarios, the total optimum injection rate was 809 ton/hr or 16.5% less from the initial injection capacity. The Well D-2 bottom hole pressure of this case was 199.1 barg at the end of the month. Figure 19 shows the pressure distribution at the end of the simulation across the reservoir. The dark blue color depicts the undisturbed region where the pressure is still in its original reservoir pressure. The impermeable faults have a significant impact on pressure propagation. As the pressure traveled during injection, the pressure bounced back when it hit the faults. It significantly magnified the pressure at a certain point in the reservoir. As a result, the interference effect was felt more severe. The occurrence of impermeable fault might realistically exist due to some interpretations. First, both faults were interpreted from gravity anomaly, lineaments and occurrence of manifestation, and lineaments on surface. Second, no loss was found in the 12-1/4” hole section of D-2 and D-3 wells. This section penetrated the east side of the Fault#2. Also, both wells' pressure transient profile indicated sealing intersecting fault boundary. Lastly, several wells drilled to the outer part of the Fault#1 and Fault#2 were not encountered any permeable zone.

6. CONCLUSION

To fulfill the expected electricity generation, Hululais Geothermal Field currently has nine production and nine reinjection wells. One of the issues that arise is the interference phenomenon of some wells, especially in reinjection wells.

According to the well completion data and the injection parameter, Well D-2 and D-3 are confirmed to have interference phenomena. It might be due to the high and narrow permeability fractured system. The transient analysis suggests that it is also bounded to the impermeable surrounding.

A simulation using isothermal semi-numerical transient software is delivered to estimate the injection capacity change due to the interference. Based on the simulation, injection capacity reduction reaches 16.5% from 969 ton/hr to 809 ton/hr for wellhead pressure 0 barg and injection temperature 40^{o}C.

An advanced method that utilizes a numerical reservoir model coupled with wellbore models, which accounts for the non-isothermal process, needs to be done to investigate the interference effect and to obtain a more accurate result.

ACKNOWLEDGEMENTS

The authors would like to express sincere gratitude to the Exploration and Exploitation Team for the resources also to the Management of PT. Pertamina Geothermal Energy, especially Fernando Pasaribu and Marihot S. P. Silaban for meaningful support to this work.

REFERENCES

Akin, S.: Design and Analysis of Multi-well Interference Tests. *Proc. World Geothermal Congress 2015, Melbourne, Australia*. (2015).

Axelsson, G.: Role and Management of Geothermal Reinjection. *Short Course on Geothermal Development and Geothermal Wells, organized by UNU-GTP and LaGeo, Santa Tecla, El Salvador*. (2012).

Bromley, C. J., Mongillo, M., and Rybach, L., 2006: Sustainable utilization strategies and promotion of beneficial environmental effects – Having your cake and eating it too. *Proceedings of the New Zealand Geothermal Workshop 2006, Auckland, New Zealand*, 5 pp. (2016).

Hastriansyah, G., Syihab, Z., Silaban, M. S. P.: Injection Wells Evaluation Using Nodal Analysis in Tompaso Geothermal Field. *Proc. Indonesia Geothermal Convention & Exhibition 2015, Jakarta Convention Center, Indonesia. (2015).*

Koestono, H., Prasetyo, I. M., Nusantara, V. D. M., Thamrin, M. H., and Kamah, M. Y.: Hydrothermal Alteration Mineralogy of Well HLS-C, Hululais Geothermal Field, Bengkulu, Indonesia. *Proc. World Geothermal Congress 2015, Melbourne, Australia*. (2015).

Meehan, D. N.: A Correlation for Water Compressibility. *Petroleum Eng, Nov 1980.* 125-26. (1980).

ISSN 2703-4275